IEEE Access
Multidisciplinary | Rapid Review | Open Access Journal

Received September 14, 2021, accepted September 21, 2021, date of publication September 27, 2021,
date of current version October 5, 2021.

Digital Object Identifier 10.1109/ACCESS.2021.3115984

Combining Surgical Navigation and 3D Printing for Less Invasive Pelvic Tumor Resections

MÓNICA GARCÍA-SEVILLA[1,2], LYDIA MEDIAVILLA-SANTOS[2,3], RAFAEL MORETA-MARTINEZ[1,2], DAVID GARCÍA-MATO[1,2], RUBÉN PÉREZ-MAÑANES[2,3], JOSÉ ANTONIO CALVO-HARO[2,3], AND JAVIER PASCAU[1,2], (Member, IEEE)

[1]Departamento de Bioingeniería e Ingeniería Aeroespacial, Universidad Carlos III de Madrid, 28911 Leganés, Madrid, Spain
[2]Instituto de Investigación Sanitaria Gregorio Marañón, 28007 Madrid, Spain
[3]Servicio de Cirugía Ortopédica y Traumatología, Hospital General Universitario Gregorio Marañón, 28007 Madrid, Spain

Corresponding author: Javier Pascau (jpascau@ing.uc3m.es)

This work was supported by the Ministerio de Ciencia e Innovación, Instituto de Salud Carlos III, and European Regional Development Fund "Una manera de hacer Europa," under Project PI18/01625.

ABSTRACT Surgical interventions for musculoskeletal tumor resection are particularly challenging in the pelvic region due to their anatomical complexity and proximity to vital structures. Several techniques, such as surgical navigation or patient-specific instruments (PSIs), have been introduced to ensure accurate resection margins. However, their inclusion usually modifies the surgical approach making it more invasive. In this study, we propose to combine both techniques to reduce this invasiveness while improving the precision of the intervention. PSIs are used for image-to-patient registration and the installation of the navigation's reference frame. We tested and validated the proposed setup in a realistic surgical scenario with six cadavers (12 hemipelvis). The data collected during the experiment allowed us to study different resection scenarios, identifying the patient-specific instrument configurations that optimize navigation accuracy. The mean values obtained for maximum osteotomy deviation or MOD (maximum distance between the planned and actual osteotomy for each simulated scenario) were as follows: for ilium resections, 5.9 mm in the iliac crest and 1.65 mm in the supra-acetabular region, and for acetabulum resections, 3.44 mm, 1.88 mm, and 1.97 mm in the supra-acetabular, ischial and pubic regions, respectively. Additionally, those cases with image-to-patient registration error below 2 mm ensured MODs of 2 mm or lower. Our results show how combining several PSIs leads to low navigation errors and high precision while providing a less invasive surgical approach.

INDEX TERMS Patient-specific instruments, pelvic tumor resection, surgical navigation, 3D printing.

I. INTRODUCTION

Pelvic tumor surgeries are challenging due to bone's morphological complexity and proximity to vital structures. In these interventions, achieving safe margins is essential as they present high local recurrence rates (70% in marginal resections and 90% in intralesional) [1], [2]. However, according to a study on simulated models of the pelvis, the probability of obtaining adequate margins following the conventional approach is only 52% (95% CI: 37-67) [3]. Consequently, several technologies have been introduced to improve resection accuracy and reduce the risk of recurrence.

The associate editor coordinating the review of this manuscript and approving it for publication was Orazio Gambino.

Computer-assisted navigation has improved precision in complex surgical settings [4]–[8]. Many studies have already proved its benefits in pelvic tumor resections [5], [7], [9], [10]. Thanks to the real-time visual feedback, tumor and adjacent anatomical structures can be identified and located accurately. The preoperative surgical plan can be easily translated to the operating room, increasing not only the resection accuracy but also the intra-operative confidence [5].

The use of navigation requires some preparation of the surgical field [4]. After the exposure of bone and tumor, a dynamic reference frame is attached to the patient's bone to account for intra-operative movements. It is then necessary to register preoperative images and patient's anatomy. This image-to-patient registration is usually performed through pair-points and surface-points matching. These points are

identified in the preoperative images and recorded during surgery on the patient using a navigation probe or pointer. The registration process is the most critical step to achieve optimal accuracy. If the software indicates an error above 1 mm, the process is generally repeated until a lower value is achieved. Additionally, correspondence between image and patient is visually verified by placing the pointer in anatomical landmarks. This verification is essential, as target registration errors can be high even if the fiducial registration error was low [11], [12]. Current registration approaches provide acceptable results, but there is still room for further improvements. Alam *et al.* [13] identify the need for registration methods providing higher efficiency, accuracy, and robustness in acceptable time frames. They also describe as a challenge the detection of reliable landmarks, either manually (which requires medical expertise and takes more time) or automatically (which requires large databases for training).

Patient-specific instruments (PSIs) are considered an alternative to surgical navigation in some scenarios [14]–[18]. They provide similar accuracy [19] while guiding the surgeons towards a predefined path without diverting their attention from the surgical field. Also, they can be manufactured with a 3D printer at a low cost [20]. However, they do not offer the information provided by surgical navigation, such as real-time image guidance, which limits their use to osteotomy assistance. Besides, PSIs correct placement cannot be verified other than subjectively [19], and incorrect positioning can lead to positive resection margins. To overcome this limitation, PSIs are commonly designed with large sizes, covering more bone surface to ensure precise fitting into the bone and, thus, accurate osteotomy guidance.

Both techniques (computer-assisted navigation and PSIs) present better accuracy than conventional procedures, but they also show some limitations. Large PSIs alter the surgical approach as their sizes imply more bone exposure [14], [21], requiring extensive dissections that increase the surgical risks. Similarly, surgical navigation modifies the intervention as the registration anatomical landmarks, which are distributed all over the hemipelvis, require the exposure of bone regions not necessarily involved in the procedure. Furthermore, the rigid fixation of the reference frame becomes cumbersome, since the setup must ensure stability [22] and avoid interference in the surgical field [23].

Therefore, it is necessary to find less invasive solutions that preserve the surgical approach but, at the same time, ensure adequate resection margins. In this paper, we propose combining both techniques to solve their limitations and benefit from the advantages they offer. We substitute the use of anatomical landmarks for registration with artificial landmarks included in the PSIs. These PSIs are designed with small sizes to limit bone exposure and manufactured with a desktop 3D printer at a low cost. The reference frame is also 3D printed and fixed to the patient with a PSI, simplifying its installation. It is also detachable, avoiding surgical interference when it is not used for navigation.

We present a study to assess the feasibility of the proposed setup, the precision of the reference frame placement in PSIs, and the system's navigation accuracy for common scenarios in pelvic tumor resections. This study has been performed in cadavers, which provide a realistic surgical simulation. The results validate this setup and show the best configuration of PSIs placement for each resection type and the navigation accuracy expected in each scenario.

II. MATERIAL AND METHODS

This section explains the methodology followed in the present study to validate each of the setup proposals. These include the design and manufacturing of PSIs and navigation reference frame with a desktop 3D printer, the reference frame's attachment to a PSI, and the use of navigation combined with small PSIs in a realistic environment. The last subsection explains the analysis performed, with data obtained from the cadaveric experiment, to evaluate the navigation system's accuracy in common surgical scenarios for pelvic tumor resection.

A. DESIGN AND VALIDATION OF THE REFERENCE FRAME ATTACHMENT

We designed a reference frame in the shape of a prism and a socket for its insertion (Fig. 1). The prism was designed with an isosceles triangular base to fit in a unique position in the socket and avoid possible rotations while presenting a simple shape. The frame included three branches with snap-fit posts for the attachment of spherical markers. We defined their positions considering the constraints for a correct localization with optical tracking (distance between markers of at least 40 mm, and differences of at least 3.5 mm between segments connecting each pair of markers) [24].

To reattach the reference frame during an intervention without the need to repeat the registration process, the reference frame's position should be maintained across insertions. To verify this assumption, we recorded the reference frame position with respect to the socket during 20 insertions. To track the socket position, we added to the design a platform with spherical markers attached. We computed the deviations of the reference frame's pose (position and orientation) in every insertion from the mean pose, decomposing these values into the translations and rotations present in every axis, defined as shown in Fig. 1.

A Polaris Spectra (NDI, Waterloo, Canada) optical tracking system was used to track the position of the reference frame and the socket. Spherical optical markers attached to the tools reflect the infrared light emitted by the device, which is then captured by the cameras to estimate their position with a trueness of 0.170 ± 0.090 mm [25].

Both the socket and the reference frame were 3D-printed on a Formlabs Form2 (Formlabs Inc., Somerville, MA, USA) 3D printer in Dental SG, a Class I biocompatible material, also used for PSIs (ISO Standard from Formlabs Vertex-Dental BV resin: EN-ISO 10993-1:2009/AC: 2010, USP Class VI). After printing, we followed three

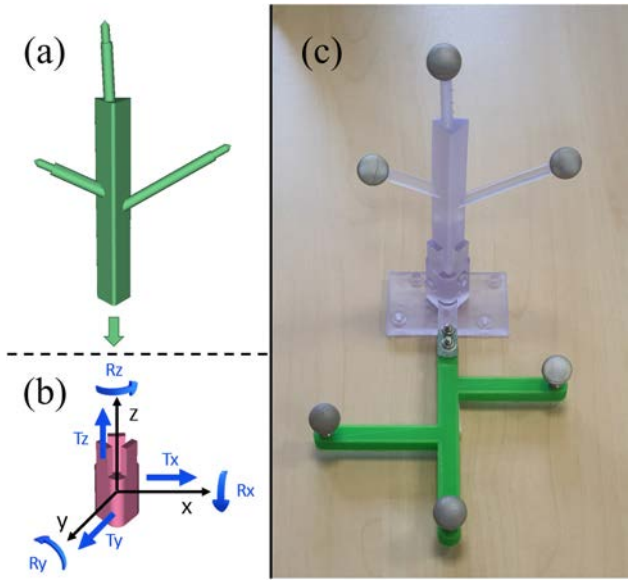

FIGURE 1. Design and validation of reference frame attachment: (a) reference frame; (b) socket and coordinate system used for the analysis; (c) setup for validation.

postprocessing steps: rinsing in isopropyl alcohol (Form Wash), removing supports, and post-curing (Form Cure) to maximize mechanical properties. When fabricating surgical guides, the surface in contact with the patient should be smooth. Hence, it is recommended to avoid the placement of supports in this area. Surgical guides can therefore be printed upside down to leave that surface free of supports. However, this means that they are placed inside the socket instead. So, it is essential to remove those supports after printing to ensure the correct insertion of the reference frame. The attachment of the spherical markers to the posts of the reference frame should also be verified after printing. In order to replicate this procedure for our experiment, the validation platform was 3D printed upside down. Supports were thoroughly removed from the socket and the reference frame. A space of 0.115 mm between the reference frame and the socket walls was included in the design, considering the 3D printer's tolerance. This way, a static insertion was achieved.

B. CADAVERIC EXPERIMENT

To validate our setup's feasibility, we conducted an experiment with a total of 6 cadaveric pelvises (three female and three male). Specimens were scanned with a CT slice thickness of 1 mm, since this value is a good compromise between accuracy and radiation exposure. Previous studies present lower thickness values [14], [19], which can provide higher precision for 3D models reconstruction but are difficult to justify in clinical practice. A model of the pelvis was extracted for every specimen through a segmentation process using thresholding. Four planes were defined in each hemipelvis presenting common osteotomy locations: iliac crest (C), supra-acetabular (S), ischial (I), and pubic (P). A PSI was designed for each osteotomy plane, presenting a small size to preserve the surgical approach. Each PSI included four pinholes to perform point-based registration [26]. C and S PSIs also contained the socket to attach the navigation reference frame. A detailed description of the PSIs design can be found in [27]. The reference frame and PSIs were 3D-printed in Dental SG resin on a Formlabs Form2 3D printer. The NDI Polaris Spectra optical tracking system was used to obtain the real-time position of the reference frame and a pointer.

We developed a custom module in 3D Slicer [28], a free and open-source multi-platform software package widely used for clinical and biomedical applications. We used the SlicerIGT kit [29] to develop our customized graphical user interface for surgical navigation and the PLUS toolkit [30] for communication with the tracker through OpenIGTLink. Our module allowed the visualization of the models for each case (pelvis, planes, PSIs, and reference frame) and recording points for analysis (Fig. 2). The user could modify the models' visibility, and the point of view could also be changed manually or by selecting one of the predefined views (lateral, superior-inferior, or anterior-posterior) shown on the left panel in Fig. 2.

Five experienced surgeons participated in the experiment placing PSIs. Surgical navigation was performed using the developed software. For each hemipelvis, the experiment consisted of the following steps (Fig. 3):

1) PSIs placement and fixation with screws
2) Attachment of the dynamic reference in the C or S PSI
3) Point-based registration with the C or S PSI
4) Recording of pinholes from the four PSIs
5) Navigation of the C or S osteotomy
6) Recording of points along the navigated osteotomy

Osteotomies were navigated to validate our setup, and points were recorded along the osteotomy to visually compare them with the plane displayed in the virtual navigation scene. We developed a questionnaire to address the main contributions and possible limitations of the proposed setup. The survey included questions regarding the reference frame installation through the PSI, the use of small PSIs, and the registration with artificial landmarks located in the PSIs. We were also interested in the difficulty perceived by surgeons regarding the placement of each PSI and the use of surgical navigation and 3D-printed PSIs. The questionnaire was developed in Google Forms and sent to the surgeons after the experiment.

C. ANALYSIS OF NAVIGATION ACCURACY

During navigation, the only feedback provided by the system regarding accuracy is the fiducial registration error. However, as Fitzpatrick *et al.* [11] concluded, this value is a poor indicator of the error found in the target region. Errors in the target area can only be verified visually by comparing the position of the tool in the patient and its position in the image or 3D model. Similarly, the placement of the PSIs can only be checked visually. Our work studies the error distribution

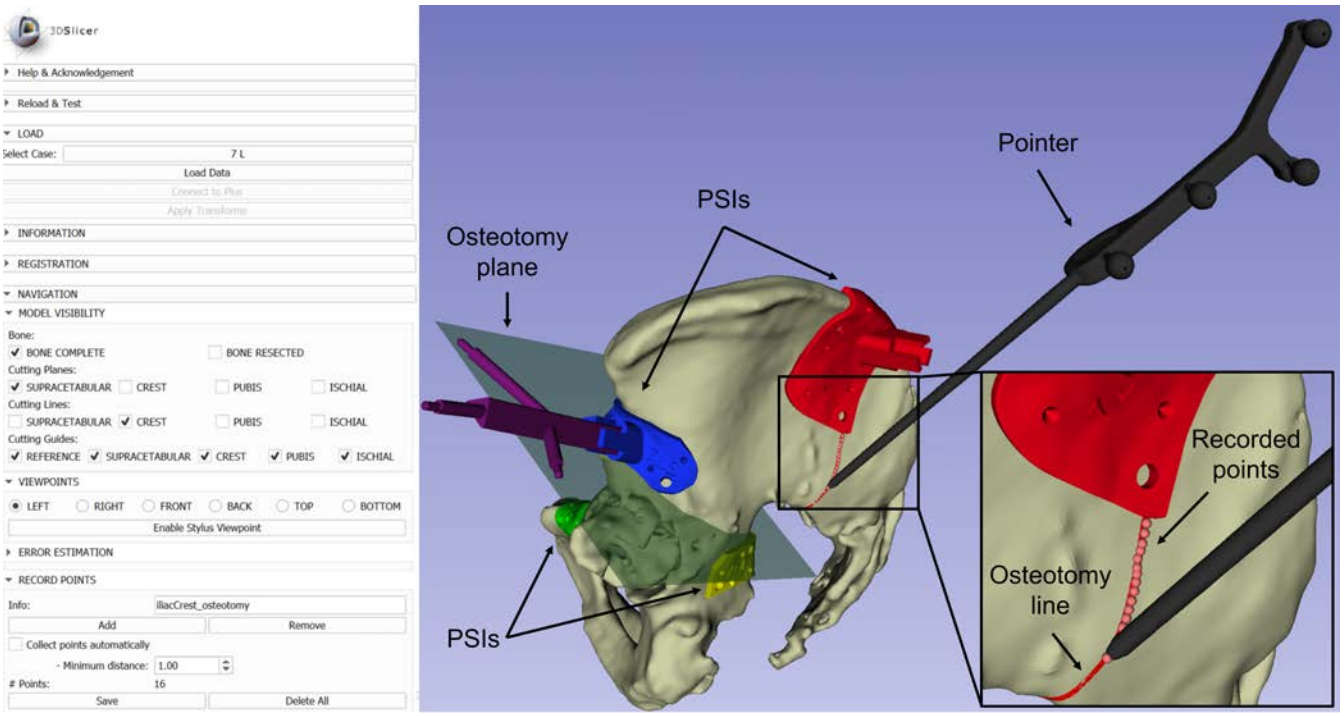

FIGURE 2. Module developed in 3D Slicer for surgical navigation of each hemipelvis.

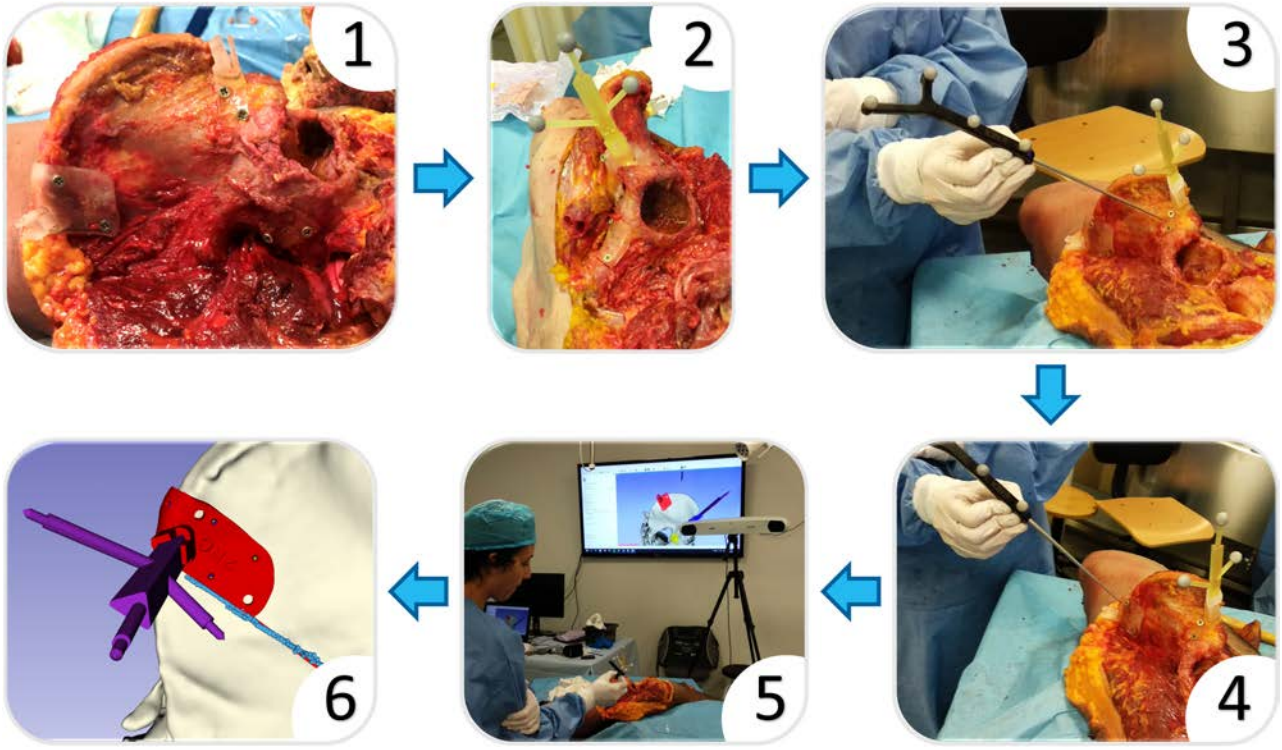

FIGURE 3. Steps followed for each case during the experiment: 1) PSIs placement and fixation; 2) reference frame placement; 3) registration; 4) recording of points in all PSIs; 5) navigation of osteotomy; 6) recording of points along the navigated osteotomy.

in the target area using the data collected intraoperatively and a postoperative CT to obtain the real locations of the PSIs. The postoperative CT was acquired for each pelvis with the PSIs still attached. The position of the PSIs was extracted from the CTs as well as the bone models. Preoperative and postoperative data of the same case were aligned using a model to model registration (based on iterative closest points algorithm [31]) between the bone models. We extracted the

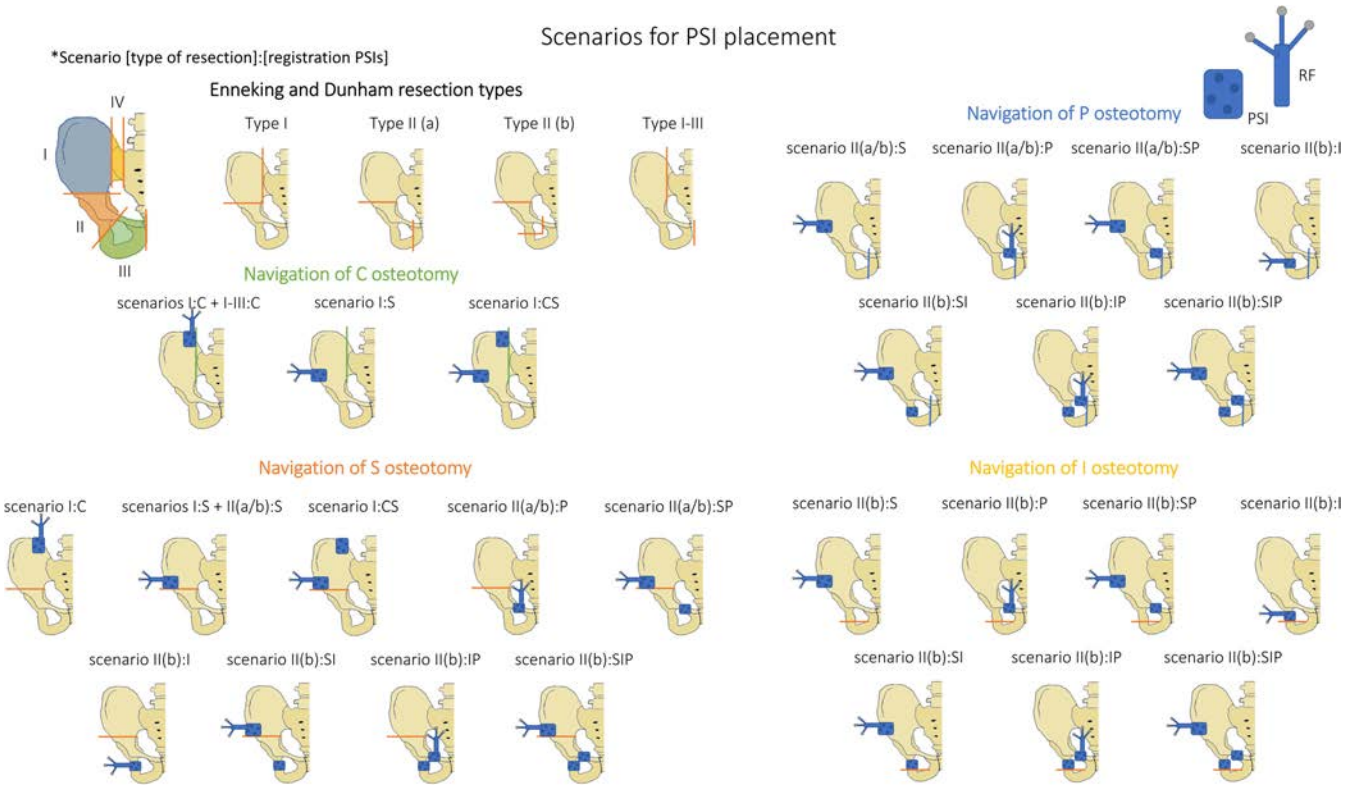

FIGURE 4. **Configurations of PSIs and reference frame (RF) for each scenario considered in the analysis. Orange lines indicate the osteotomies involved in each configuration.**

transformation between preoperative and postoperative PSIs as explained in [27]. These transformations allowed us to characterize the displacement with respect to the planning position.

The data collected during the experiment (recorded points in all PSIs), together with the pre- and postoperative data, were used to analyze the accuracy provided by the navigation system. Our analysis considered different scenarios, defined according to the pelvic tumor resection classification by Enneking and Dunham [32]. In each scenario, the PSIs and the reference frame are placed in different locations. Fig. 4 presents the resulting configurations considered for each of these scenarios.

All these configurations could be analyzed for every specimen by performing the following procedure. As the landmarks for all PSIs were collected in every hemipelvis, we can choose the points from one (or more) PSIs to simulate a specific scenario where those points are used for registration with the virtual plan. The virtual scene will then show the osteotomy planes at a particular position, and those planes would be used to guide the osteotomies. However, this position displayed by the navigation scene may not correspond to the correct one due to registration errors. These registration errors can arise from navigation inaccuracies, fiducial localization errors, and incorrect positioning of PSIs. As we have the real position of the PSIs from the postoperative CT (which represents the real scene), we can register the navigation scene with the real scene using the collected landmarks from all PSIs. That way, we can compare the position of the osteotomies according to that particular navigation scene with their real position. Therefore we can quantify the navigation error for that scenario. Fig. 5 represents these steps graphically. The diagram uses as an example the scenario where registration is performed using only the landmarks from the S PSI.

Following this procedure, we analyzed the errors in every configuration. As mentioned earlier, we can identify two sources of error in each scenario: PSI placement and navigation. As placement errors have already been analyzed by García-Sevilla *et al.* [27], here we focus on the errors introduced only by navigation and the ones resulting from the combination of both sources (total error). Total errors result from navigation errors (inaccuracies introduced by the tracking device or the user when recording the registration points) and incorrect placement of the PSIs, making the virtual plan differ from the real scene. In order to extract the navigation errors separately, we can assume PSIs were correctly placed. Therefore, we can take the real scene as the virtual plan. Fig. 5 represents the steps for the extraction of the two error types. The diagram shows how virtual and real scenes coincide when computing the navigation error but differ for the computation of the total error.

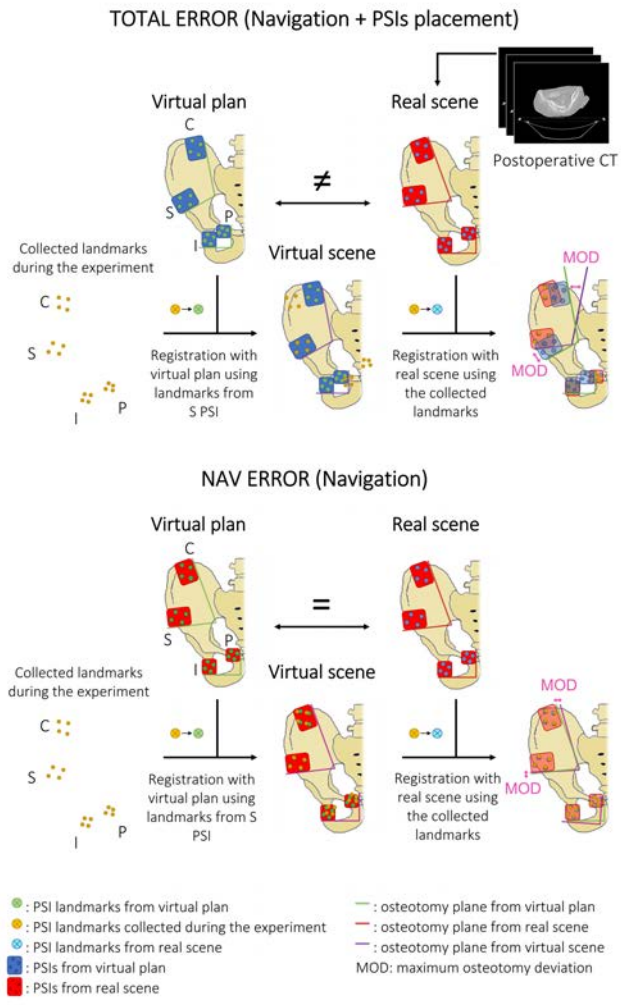

FIGURE 5. Representation of the steps followed to analyze total and navigation errors in every configuration of PSIs, illustrated with the scenario in which only S PSI is used for registration.

We measured the maximum osteotomy deviation (MOD) for each configuration. That is the maximum distance between the osteotomy that would be performed based on the navigation scene and the osteotomy defined in the virtual plan. To compute this distance, we first extracted the intersection of the osteotomy plane in the virtual plan with the bone, generating a 3D model (point cloud). Then we transformed that osteotomy plane to the real scene to place it where the cut would be performed in that specific scenario. Once again, we extracted the intersection of that plane with the bone. Finally, we computed the maximum distance between both models. For that, we computed the distance of every point in one intersection model to its closest point in the other intersection model. The MOD was defined as the maximum distance obtained from this computation. The Supplementary Material includes a graphical representation of the procedure.

As navigation can be used for other purposes apart from guiding the osteotomies (for instance, to identify the tumor and other anatomical structures), we also computed the error distribution across the bone surface. First, all data was centered and aligned with the RAS (Right, Anterior, Superior) coordinate system. Then, we extracted the transform between virtual and real scenes for every case and applied it to a pelvis model used as a reference. We measured the distances between corresponding points of the original and the transformed models. Finally, we computed the mean error of every surface point for each configuration.

TABLE 1. Descriptive statistics of translation (T) and rotation (R) errors in every axis (x, y, z) for the insertion of the reference frame in the socket.

	Tx	Ty	Tz	Rx	Ry	Rz
Mean	0.02	0.02	0.02	0.15	0.22	0.07
SD	0.01	0.02	0.02	0.12	0.14	0.04
Max.	0.05	0.05	0.09	0.50	0.57	0.20

SD = standard deviation

III. RESULTS

A. DESIGN AND VALIDATION OF THE REFERENCE FRAME ATTACHMENT

The reference frame was inserted 20 times in the socket. We recorded the pose for each insertion and computed the deviations from the mean (calculated from the 20 repetitions) to report the placement precision. The resulting mean, standard deviation, and maximum deviation values for translations and rotations are presented in Table 1 for each axis defined in Fig. 1.

Translations present a mean deviation of 0.02 mm and a standard deviation of 0.02 mm or lower in all axes. Maximum deviations in translations are below 0.10 mm. Mean rotations are below 0.25°, with a standard deviation below 0.15° and maximum rotations below 0.6°. The direction of the insertion (z-axis) presents the highest translation and the lowest rotations.

B. CADAVERIC EXPERIMENT

PSIs were rigidly fixed to the bone with screws, and the navigation was performed successfully. The reference frame was easily inserted in all PSIs, and it was correctly tracked during the experiment without interfering with the procedure. The surgeons were able to navigate the osteotomies using the tracked tools and the navigation system.

The Supplementary Material collects valuable feedback from the surgeons involved in the experiment. Surgeons agree that the use of both techniques requires training but presents an advantage due to the reduced sizes of PSIs, the ability to attach and detach the reference frame, and the substitution of anatomical with artificial landmarks for registration. They also agree that having a tool to verify PSIs placement would be very valuable.

C. ANALYSIS OF NAVIGATION ACCURACY: MAXIMUM OSTEOTOMY DEVIATION

For every hemipelvis, we extracted the MOD in each region (C, S, I and P) with every configuration presented in Fig. 4.

TABLE 2. Mean and standard deviation of the maximum osteotomy deviations in each configuration (values are in mm). The lowest values for each osteotomy are presented in bold.

Ost.	Error Type	Metric	PSIs used for registration								
			C	S	I	P	CS	SI	SP	IP	SIP
C	TOTAL	Mean	8.18	7.48			**5.90**				
		SD	4.01	4.79			3.84				
	NAV	Mean	2.58	5.64			**1.29**				
		SD	2.23	2.50			1.17				
S	TOTAL	Mean	9.03	4.73	4.95	6.12	**1.65**	4.48	3.46	9.70	**3.44**
		SD	7.67	4.37	3.64	6.62	0.93	3.15	1.90	9.31	2.33
	NAV	Mean	4.57	2.60	4.60	6.19	**0.76**	1.45	2.86	2.06	**1.32**
		SD	3.56	1.29	3.14	4.57	0.33	1.03	0.74	1.46	0.75
I	TOTAL	Mean		4.27	3.47	9.83		2.12	3.64	4.17	**1.88**
		SD		1.80	2.34	6.09		0.83	1.67	2.26	0.64
	NAV	Mean		1.58	1.36	8.99		1.02	2.95	1.44	**0.72**
		SD		0.59	0.65	6.10		0.91	1.72	0.87	0.48
P	TOTAL	Mean		2.29	4.48	3.13		4.18	2.47	2.48	**1.97**
		SD		1.36	4.96	1.60		3.63	1.41	1.62	1.16
	NAV	Mean		1.10	4.02	1.37		2.22	0.83	0.93	**0.66**
		SD		0.81	3.68	0.57		1.85	0.56	0.70	0.45

C = iliac crest, S = supra-acetabular, I = ischial, P = pubic, PSIs = patient-specific instruments, SD = standard deviation, NAV = navigation, Ost. = osteotomy

TABLE 3. Registration errors for maximum osteotomy deviations (MODs) below 2 mm and MODs for registration errors below 2 mm. The table presents the number of cases used, mean, standard deviation, and 75th quartile for each resection type with their optimal registration configurations.

		Type I C & S	Type II(a) S & P	Type II(b) S, I & P
Registration errors for MODs <2 mm	Number of cases	11	12	7
	Mean	1.90	2.54	2.46
	SD	0.99	1.32	1.40
	75%	2.38	3.67	4.07
MODs for registration errors <2 mm	Number of cases	9	8	7
	Mean	1.73	1.23	1.32
	SD	2.46	0.97	0.99
	75%	2.01	1.56	1.70

C = iliac crest, S = supra-acetabular, I = ischial, P = pubic, SD = standard deviation, MOD = maximum osteotomy deviation

Table 2 shows the mean and standard deviation values in each osteotomy plane for the different combinations of PSIs used for registration. The results are divided into ''Total'' errors (which result from placement and navigation errors) and ''Nav'' errors (which are only a result of navigation errors).

The results demonstrate how using multiple PSIs for registration improves navigation accuracy, providing the lowest deviation errors. For the total errors in C and S osteotomies, using both PSIs for registration gives MODs with a mean value of 5.90 mm in C and 1.65 mm in S. For navigation errors, we can observe the same behavior, where registration with C and S PSIs gives a mean error of 1.29 mm in C and 0.76 mm in S. Therefore, when performing type I resections, it is best to use both PSIs. For type I-III resections, deviations depend only on the correct placement in C, where the mean error is 8.18 mm.

Using S and P PSIs shows the highest accuracy for type II(a) resections, with mean values of 3.46 mm in S and 2.47 mm in P for total errors and 2.86 mm and 0.83 mm for navigation errors. For type II(b) resections, MODs present the lowest values when using S, I, and P PSIs for registration. The mean values for the total errors are 3.44 mm in S, 1.88 mm in I, and 1.97 mm in P. For navigation errors, these values are 1.32 mm, 0.72 mm, and 0.66 mm, respectively.

When using multiple PSIs, high patient-image registration errors can be indicative of incorrect placements. In these situations, PSIs can be repositioned until a lower error is achieved. As navigation accuracy highly depends on the correct positioning of the PSIs, low registration errors can be used to ensure precise navigated osteotomies. To determine which registration values are acceptable for navigation, we have selected from total and navigation data those scenarios using multiple PSIs for registration. In particular, we have chosen those cases presenting the optimal configuration in each resection (registration with C and S PSIs for type I, with S and P PSIs for type II(a), and with S, I, and P PSIs for type II(b)). From this data, we have extracted those cases where MODs are below 2 mm, and we have analyzed their corresponding registration errors. We have also obtained cases with registration errors below 2 mm to identify their MOD. The results for each analysis are presented in Table 3.

In cases with MOD below 2 mm, most registration errors are between 1 and 4 mm. Mean values are lower than 2 mm in type I resections and below 2.6 mm for type II. 75% of the cases in type I resections present registration errors below 2.38 mm, and below 3.67 mm and 4.07 mm in type II(a) and type II(b), respectively. Registration errors below 2 mm present MODs of 2 mm or lower in 75% of the cases.

Therefore, in these configurations, registration errors lower or equal to 2 mm ensure a precise navigated osteotomy in most cases, with maximum deviations below 2 mm.

D. ANALYSIS OF NAVIGATION ACCURACY: ERROR DISTRIBUTION

Apart from measuring the MOD, we analyzed the navigation error distribution across the bone's surface for each configuration. The results are presented in Fig. 6, where one of the hemipelvis from the study is used to represent the distances computed with the data from all cases. These values indicate the errors we would find in all the hemipelvis, assuming a correct placement of PSIs.

The results show how the error is lower in the areas close to the PSIs used for registration. When using multiple PSIs, errors are reduced not only in the PSIs location but also in the area between them. The configuration CS (registration with C and S) presents the best navigation results in the ilium region with errors below 2 mm. As for the acetabular region, the SIP configuration presents errors below 2 mm, and below 5 mm in all the hemipelvis.

IV. DISCUSSION

The resection of tumors located in the pelvis becomes very challenging due to the complex morphology of the bone and the proximity to vital structures. Tools such as surgical navigation or PSIs have shown improvements in precision, but they also result in more invasive approaches. In this study, we introduce a new, less invasive solution combining both

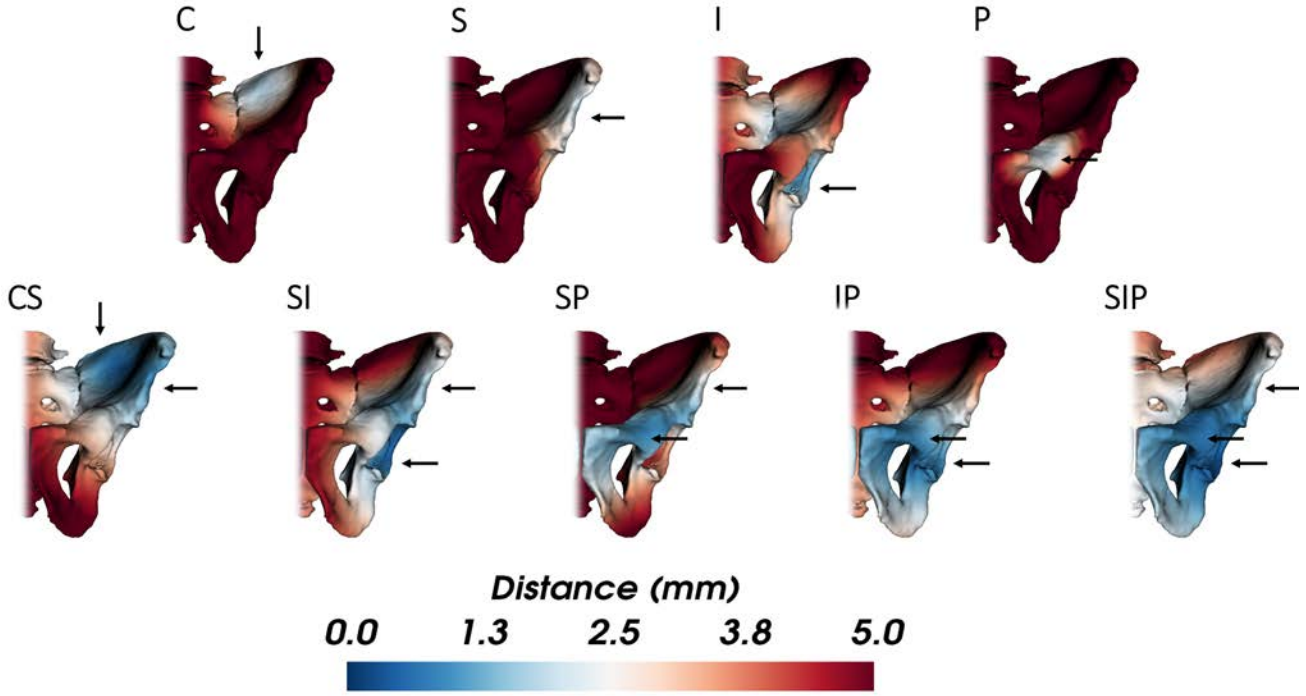

FIGURE 6. Navigation error distribution for every configuration of PSIs considered for the analysis. Arrows indicate the position of the PSIs.

tools. The proposed setup has been tested and validated in a realistic environment with cadavers.

As an alternative to the fixation to the patient's bone, we propose using PSIs for an easier and more convenient installation of the navigation's reference frame, which can be attached only when necessary. Our study has evaluated the repeatability of its placement, which avoids performing the registration for every new insertion. The identified placement error was below 0.1 mm in translation and 0.6° in rotation. These values are negligible considering the error introduced by the optical tracking system [33].

PSIs also become a valuable tool for registration since artificial landmarks included in the PSIs replace anatomical landmarks and surface-points, reducing bone exposure and solving some of their limitations [5], [23], [34]. Besides, they are easier to identify, reducing intra- and interobserver variability in the registration process. Previous studies have also replaced anatomical landmarks with bone-mounted fiducial markers improving registration results [9], [35]. However, these solutions usually require the implantation of titanium pins prior to the preoperative CT and are more invasive. Nevertheless, if registration relies on artificial landmarks located in the PSIs, the navigation accuracy is highly dependent on their correct placement, which is challenging to ensure [27]. If registration is computed from a single PSI, low registration errors can be misleading. However, when using multiple PSIs, high registration errors may indicate incorrect placements that can then be rectified. Hence, low registration errors can ensure precise navigation. We have identified the registration errors associated with precise osteotomies when using multiple PSIs. The results show that, in most cases, 2 mm or lower registration errors ensure MODs below 2 mm.

PSIs positions depend on the surgical scenario and the planned osteotomies, but thanks to a novel methodology, we could analyze different PSI and osteotomy combinations in a single specimen. During the experiment, PSIs were placed in the four most common osteotomy regions (C, S, I, and P). We recorded the position of all the artificial landmarks present in the PSIs. From the data collected during the experiment with the six cadaveric specimens, we analyzed the system's precision when performing registration with different combinations of PSIs for type I, type II, and type I-III resections [32]. The results presented in Table 2 and Fig. 6 demonstrate how using multiple PSIs for registration always offers the highest precision in the area of interest. These results align with previous studies from Fitzpatrick *et al.* [11] and West *et al.* [12], who studied how the configuration of the landmarks used for registration affects the error distribution in the navigated surgical field. They found that low errors can be achieved in the target region if fiducials are widely spread and surrounding the area. Ideally, the target would be placed in the centroid of the markers. Hence, using multiple PSIs (composing a set of landmarks spread and surrounding the navigation area) presents lower errors. When using a single PSI for registration, as all registration landmarks are distributed in the PSI, the errors in that area are low. Inaccuracies in the localization of fiducials can result in small translations and rotations close to the landmarks. However, these errors increase with distance, and so we obtain high errors far from the PSI used for registration.

Therefore, if we consider the scenarios presented in Fig. 4, both C and S PSIs should be used for type I resections, S, I, and P should be combined for type II or, if the ischial osteotomy is not performed, only S and P. For type I-III resections, as the PSI in C is the only one used, incorrect placement can cause high navigation errors. Therefore, in this case, it would be advisable to use additional PSIs in the iliac crest or the symphysis to reduce errors and verify correct placement. In this and any other scenarios, PSIs can be used exclusively for registration, avoiding their fixation to the bone.

The proposed setup was tested in cadavers following a realistic surgical approach, where surgeons successfully placed PSIs and navigated the osteotomies. Overall feedback from the surgeons was very positive. They all agreed that the setup proposal, including the reduced size of PSIs, the reference frame's installation, and the use of artificial landmarks, presented an advantage compared to conventional procedures or using either technology independently (Supplementary Material). They also concurred that navigation requires more training and experience than PSIs. However, there were some discrepancies regarding the difficulty in PSI placement for each region. Although C PSIs are the ones presenting higher placement errors followed by S PSIs [27], some surgeons found the placement more challenging in other regions whereas others considered all regions equally tricky. These incoherent results highlight the difficulty of identifying erroneous placements, a significant limitation of PSIs. Surgeons agreed on the usefulness of a verification tool for PSIs placement, which would avoid high errors during guidance. In our setup, registration errors can be used for this purpose.

The MODs obtained considering placement errors are similar to those obtained in other studies using only surgical navigation or PSIs. Wong *et al.* [19] studied the mean MODs in supra-acetabular and partial-acetabular resections with both techniques, obtaining errors of 3.6 mm with surgical navigation and 2.6 mm with large and multiplanar PSIs. Sallent *et al.* [14] used PSIs in 5 cadaveric specimens obtaining mean MODs of 5 mm in the sacroiliac joint, 4 and 3.6 mm in the supra-acetabular region, 2.2 mm in the ischial osteotomies, and 0.8 and 1 mm in pubic osteotomies. Fehlberg *et al.* [23] obtained a median deviation of 3.3 mm in a series of 13 patients.

Our setup can be replicated by following the indications given for the design of the surgical guides [27] and the fabrication of the 3D-printed tools. If Dental SG resin is used for 3D printing, it should be stored following the manufacturer's indications (a cool, dry place out of direct sunlight in containers at 10 – 25 °C). The orientation of the surgical guides should be carefully studied to ensure smoothness in the surface in contact with the patient. Supports added inside the socket or in the reference frame should be thoroughly removed, and the correct insertion of the reference frame in the socket and the optical markers in the posts should be verified before use. Models of the reference frame and socket are available at https://dx.doi.org/10.21227/zcbr-k673. During navigation, it is essential to ensure adequate lightning conditions in the surgical field. Materials presenting similar properties to the optical markers could reflect the infrared light emitted by the optical tracker and result in tracking errors.

V. CONCLUSION

To conclude, we have proposed and validated a new setup for pelvic tumor resections using surgical navigation and PSIs. The novelty of our study relies upon the fact that both techniques, 3D printing and image-guided surgery, are combined to provide a less invasive setup. This invasiveness is reduced by using small PSIs, which also act as artificial landmarks. We have also presented a new and more convenient installation of the dynamic reference frame using a socket included in the PSI. This installation has demonstrated repeatability, which allows the removal of the reference frame without the need to repeat the registration step every time it is reinserted.

A realistic experiment on cadavers allowed us to describe the optimal PSIs configuration in three different resection scenarios. We computed the MODs for all cases and identified the registration errors minimizing these deviations. Additionally, we studied the distribution of the navigation error in the target regions, which to our knowledge has not been previously analyzed. We can conclude that the best results are achieved when at least two PSIs are used surrounding the area of interest. Our results show how, with our setup, correct PSI placements lead to low navigation errors and high accuracy while providing a less invasive surgical approach.

REFERENCES

[1] T. Ozaki, S. Flege, M. Kevric, N. Lindner, R. Maas, G. Delling, R. Schwarz, A. R. von Hochstetter, M. Salzer-Kuntschik, W. E. Berdel, H. Jürgens, G. U. Exner, P. Reichardt, R. Mayer-Steinacker, V. Ewerbeck, R. Kotz, W. Winkelmann, and S. S. Bielack, "Osteosarcoma of the pelvis: Experience of the cooperative osteosarcoma study group," *J. Clin. Oncol.*, vol. 21, no. 2, pp. 334–341, Jan. 2003, doi: 10.1200/JCO.2003.01.142.

[2] B. Fuchs, N. Hoekzema, D. R. Larson, C. Y. Inwards, and F. H. Sim, "Osteosarcoma of the pelvis: Outcome analysis of surgical treatment," *Clin. Orthopaedics Rel. Res.*, vol. 467, no. 2, pp. 510–518, Feb. 2009.

[3] O. Cartiaux, P.-L. Docquier, L. Paul, B. G. Francq, O. H. Cornu, C. Delloye, B. Raucent, B. Dehez, and X. Banse, "Surgical inaccuracy of tumor resection and reconstruction within the pelvis: An experimental study," *Acta Orthopaedica*, vol. 79, no. 5, pp. 695–702, Jan. 2008.

[4] K. C. Wong, X. Niu, H. Xu, Y. Li, and S. Kumta, "Computer navigation in orthopaedic tumour surgery," *Adv. Experim. Med. Biol.*, vol. 1093, pp. 315–326, Oct. 2018.

[5] P. S. Young, H. Findlay, J. T. S. Patton, and A. Mahendra, "(iii) Computer assisted navigation in musculoskeletal oncology," *Orthopaedics Trauma*, vol. 28, no. 5, pp. 294–302, Oct. 2014, doi: 10.1016/j.mporth.2014.08.002.

[6] K. Cleary and T. M. Peters, "Image-guided interventions: Technology review and clinical applications," *Annu. Rev. Biomed. Eng.*, vol. 12, no. 1, pp. 119–142, Jul. 2010.

[7] K. C. Wong, S. M. Kumta, K. H. Chiu, G. E. Antonio, P. Unwin, and K. S. Leung, "Precision tumour resection and reconstruction using image-guided computer navigation," *J. Bone Joint Surgery. Brit.*, vol. 89-B, no. 7, pp. 943–947, Jul. 2007.

[8] R. Moreta-Martinez, J. A. Calvo-Haro, R. Pérez-Mañanes, M. García-Sevilla, L. Mediavilla-Santos, and J. Pascau, "Desktop 3D printing: Key for surgical navigation in acral tumors?" *Appl. Sci.*, vol. 10, no. 24, 2020, doi: 10.3390/app10248984.

[9] T. Hüfner, M. Kfuri, M. Galanski, L. Bastian, M. Loss, T. Pohlemann, and C. Krettek, "New indications for computer-assisted surgery: Tumor resection in the pelvis," *Clin. Orthopaedics Rel. Res.*, vol. 426, pp. 219–225, Sep. 2004.
[10] L. Jeys, G. S. Matharu, R. S. Nandra, and R. J. Grimer, "Can computer navigation-assisted surgery reduce the risk of an intralesional margin and reduce the rate of local recurrence in patients with a tumour of the pelvis or sacrum?" *Bone Joint J.*, vols. 95–B, no. 10, pp. 1417–1424, Oct. 2013.
[11] J. M. Fitzpatrick, J. B. West, and C. R. Maurer, "Predicting error in rigid-body point-based registration," *IEEE Trans. Med. Imag.*, vol. 17, no. 5, pp. 694–702, Oct. 1998.
[12] J. B. West, J. M. Fitzpatrick, S. A. Toms, C. R. Maurer, Jr., and R. J. Maciunas, "Fiducial point placement and the accuracy of point-based, rigid body registration," *Neurosurgery*, vol. 48, no. 4, pp. 810–817, Apr. 2001, doi: 10.1097/00006123-200104000-00023.
[13] F. Alam, S. U. Rahman, S. Ullah, and K. Gulati, "Medical image registration in image guided surgery: Issues, challenges and research opportunities," *Biocybernetics Biomed. Eng.*, vol. 38, no. 1, pp. 71–89, Oct. 2018.
[14] A. Sallent, M. Vicente, M. M. Reverté, A. Lopez, A. Rodríguez-Baeza, M. Pérez-Domínguez, and R. Velez, "How 3D patient-specific instruments improve accuracy of pelvic bone tumour resection in a cadaveric study," *Bone Joint Res.*, vol. 6, no. 10, pp. 577–583, Oct. 2017.
[15] T. M. Wong, J. Jin, T. W. Lau, C. Fang, C. H. Yan, K. Yeung, M. To, and F. Leung, "The use of three-dimensional printing technology in orthopaedic surgery: A review," *J. Orthopaedic Surgery*, vol. 25, no. 1, pp. 1–7, 2017.
[16] O. Cartiaux, L. Paul, B. G. Francq, X. Banse, and P.-L. Docquier, "Improved accuracy with 3D planning and patient-specific instruments during simulated pelvic bone tumor surgery," *Ann. Biomed. Eng.*, vol. 42, no. 1, pp. 205–213, Jan. 2014.
[17] T. Jentzsch, L. Vlachopoulos, P. Fürnstahl, D. A. Müller, and B. Fuchs, "Tumor resection at the pelvis using three-dimensional planning and patient-specific instruments: A case series," *World J. Surgical Oncol.*, vol. 14, no. 1, pp. 1–12, Dec. 2016, doi: 10.1186/s12957-016-1006-2.
[18] M. A. Hafez and K. Moholkar, "Patient-specific instruments: Advantages and pitfalls," *SICOT-J*, vol. 3, p. 66, Dec. 2017.
[19] K.-C. Wong, K.-Y. Sze, I. O.-L. Wong, C.-M. Wong, and S.-M. Kumta, "Patient-specific instrument can achieve same accuracy with less resection time than navigation assistance in periacetabular pelvic tumor surgery: A cadaveric study," *Int. J. Comput. Assist. Radiol. Surgery*, vol. 11, no. 2, pp. 307–316, Feb. 2016.
[20] M. Narita, T. Takaki, T. Shibahara, M. Iwamoto, T. Yakushiji, and T. Kamio, "Utilization of desktop 3D printer-fabricated 'cost-effective' 3D models in orthognathic surgery," *Maxillofacial Plastic Reconstructive Surgery*, vol. 42, no. 1, pp. 1–7, 2020.
[21] F. Gouin, L. Paul, G. A. Odri, and O. Cartiaux, "Computer-assisted planning and patient-specific instruments for bone tumor resection within the pelvis: A series of 11 patients," *Sarcoma*, vol. 2014, Jul. 2014, Art. no. 842709.
[22] K. C. Wong and S. M. Kumta, "Joint-preserving tumor resection and reconstruction using image-guided computer navigation," *Clin. Orthopaedics Rel. Res.*, vol. 471, no. 3, pp. 762–773, 2013.
[23] S. Fehlberg, S. Eulenstein, T. Lange, D. Andreou, and P. U. Tunn, "Computer-assisted pelvic tumor resection: Fields of application, limits, and perspectives," *Recent Results Cancer Res.*, vol. 179, pp. 169–182, Oct. 2009.
[24] A. J. V. Brown, A. Uneri, T. S. D. Silva, A. Manbachi, and J. H. Siewerdsen, "Design and validation of an open-source library of dynamic reference frames for research and education in optical tracking," *J. Med. Imag.*, vol. 5, no. 2, pp. 1–8, 2018, doi: 10.1117/1.JMI.5.2.021215.
[25] R. Elfring, M. de la Fuente, and K. Radermacher, "Assessment of optical localizer accuracy for computer aided surgery systems," *Comput. Aided Surgery*, vol. 15, nos. 1–3, pp. 1–12, Feb. 2010, doi: 10.3109/10929081003647239.
[26] K. S. Arun, T. S. Huang, and S. D. Blostein, "Least-squares fitting of two 3-D point sets," *IEEE Trans. Pattern Anal. Mach. Intell.*, vol. PAMI-9, no. 5, pp. 698–700, Sep. 1987.
[27] M. García-Sevilla, L. Mediavilla-Santos, M. T. Ruiz-Alba, R. Pérez-Mañanes, J. A. Calvo-Haro, and J. Pascau, "Patient-specific desktop 3D-printed guides for pelvic tumour resection surgery: A precision study on cadavers," *Int. J. Comput. Assist. Radiol. Surgery*, vol. 16, no. 3, pp. 397–406, Mar. 2021, doi: 10.1007/s11548-021-02322-3.
[28] A. Fedorov, R. Beichel, J. Kalpathy-Cramer, J. Finet, J. C. Fillion-Robin, S. Pujol, C. Bauer, D. Jennings, F. Fennessy, M. Sonka, J. Buatti, S. Aylward, J. V. Miller, S. Pieper, and R. Kikinis, "3D Slicer as an image computing platform for the quantitative imaging network," *Magn. Reson. Imag.*, vol. 30, no. 9, pp. 1323–1341, 2012, doi: 10.1016/j.mri.2012.05.001.
[29] T. Ungi, A. Lasso, and G. Fichtinger, "Open-source platforms for navigated image-guided interventions," *Med. Image Anal.*, vol. 33, pp. 181–186, Oct. 2016.
[30] A. Lasso, T. Heffter, A. Rankin, C. Pinter, T. Ungi, and G. Fichtinger, "PLUS: Open-source toolkit for ultrasound-guided intervention systems," *IEEE Trans. Biomed. Eng.*, vol. 61, no. 10, pp. 2527–2537, Oct. 2014.
[31] P. J. Besl and D. N. McKay, "A method for registration of 3-D shapes," *IEEE Trans. Pattern Anal. Mach. Intell.*, vol. 14, no. 2, pp. 239–256, Feb. 1992.
[32] W. F. Enneking and W. K. Dunham, "Resection and reconstruction for primary neoplasms involving the innominate bone," *J. Bone Joint Surgery*, vol. 60, no. 6, pp. 731–746, Sep. 1978.
[33] R. Khadem, C. C. Yeh, M. Sadeghi-Tehrani, M. R. Bax, J. A. Johnson, J. N. Welch, E. P. Wilkinson, and R. Shahidi, "Comparative tracking error analysis of five different optical tracking systems," *Comput. Aided Surgery*, vol. 5, no. 2, pp. 98–107, Jan. 2000.
[34] T. Y. C. So, Y.-L. Lam, and K.-L. Mak, "Computer-assisted navigation in bone tumor surgery: Seamless workflow model and evolution of technique," *Clinical Orthopaedics Rel. Res.*, vol. 468, no. 11, pp. 2985–2991, 11 2010.
[35] D. García-Mato, S. Ochandiano, M. García-Sevilla, C. Navarro-Cuéllar, J. V. Darriba-Allés, R. García-Leal, J. A. Calvo-Haro, R. Pérez-Mañanes, J. I. Salmerón, and J. Pascau, "Craniosynostosis surgery: Workflow based on virtual surgical planning, intraoperative navigation and 3D printed patient-specific guides and templates," *Sci. Rep.*, vol. 9, no. 1, p. 17691, Dec. 2019, doi: 10.1038/s41598-019-54148-4.

MÓNICA GARCÍA-SEVILLA received the B.S. degree in audiovisual systems engineering from Universidad Carlos III de Madrid, Spain, in 2014, and the M.Sc. degree in artificial vision from Universidad Rey Juan Carlos de Madrid, Spain, in 2016. She is currently pursuing the Ph.D. degree in biomedical science and technology with Universidad Carlos III de Madrid. She did an internship at the Department of Computer Science, Malone's Center for Engineering in Healthcare, Johns Hopkins University, Baltimore, MD, USA, in 2019. Her research interests include computer-assisted surgery, 3D printing, augmented and virtual reality, and surgical skills assessment.

LYDIA MEDIAVILLA-SANTOS received the Medical degree from Universidad Complutense de Madrid, Madrid, Spain, in 2007. She did her medical residency at Hospital General Universitario Gregorio Marañón, Madrid. Since 2008, she has been working with the Department of Orthopedic Surgery and Traumatology, Hospital General Universitario Gregorio Marañón, where she has been with the Department of Surgical Oncology, since 2015. She is currently a Trauma and Orthopedic Surgeon specializing in orthopedic oncology surgery. She is also a Researcher with the Instituto de Investigación Sanitaria Gregorio Marañón specialized in innovation and medical assistive technology.

RAFAEL MORETA-MARTINEZ received the bachelor's degree in biomedical engineering and the master's degree in multimedia and communications from Universidad Carlos III de Madrid, Spain, in 2015 and 2016, respectively, where he is currently pursuing the Ph.D. degree in biomedical science and technology. He worked as a Researcher with the Applied Chest Imaging Laboratory in Brigham and Women's Hospital, Boston, MA, USA, in 2018, for a period of one year. His work focused on deep learning applied to medical image segmentation. His research interests include image-guided surgery, augmented reality, medical 3D printing, and deep learning applied to medical imaging.

DAVID GARCÍA-MATO received the B.S. degree in biomedical engineering and the M.Sc. degree in multimedia and communications from Universidad Carlos III de Madrid, Spain, in 2015 and 2016, respectively, where he is currently pursuing the Ph.D. degree in biomedical science and technology. He worked as a Researcher with the Laboratory for Percutaneous Surgery, Queen's University, Kingston, ON, Canada, in 2017, and Sheikh Zayed Institute for Pediatric Surgical Innovation, Children's National Hospital, Washington, DC, USA, in 2019. His research interests include medical imaging and computer-assisted interventions.

RUBÉN PÉREZ-MAÑANES received the Medical degree from Universidad Autónoma de Madrid, Spain, in 2004, and the Ph.D. degree from Universidad Complutense de Madrid, Spain, in 2010.

He is currently a Trauma and Orthopedic Surgeon specialized in oncologic and reconstructive surgery and a Researcher with the Instituto de Investigación Sanitaria Gregorio Marañón. He is specialized in innovation and medical assistive technology. He is also an Associate Teacher in ciencias de la salud with Universidad Complutense de Madrid. He co-founded the 3D Printing Unit, Hospital General Universitario Gregorio Marañón. He is also the Co-Director of Curso Anual de Actualización en Tumores del Aparato Locomotor and of Jornadas de Actualización en Impresión 3D Médica Hospitalaria.

JOSÉ ANTONIO CALVO-HARO received the Medical and Ph.D. degrees from Universidad Complutense de Madrid, Madrid, Spain, in 2001 and 2007, respectively.

He did his Medical Residency at Hospital General Universitario Gregorio Marañón, Madrid. He is currently a Researcher with the Instituto de Investigación Sanitaria Gregorio Marañón specialized in innovation and medical assistive technology and an Associate Teacher in ciencias de la salud with Universidad Complutense de Madrid. He is also a Trauma and Orthopedic Surgeon specialized in oncologic and reconstructive surgery. He is also a member of the Unidad de Referencia Nacional (CSUR) in Sarcomas. He is also one of the founders and co-directors of the 3D Printing Unit, Hospital General Universitario Gregorio Marañón, the Co-Director of Curso Anual de Actualización en Tumores del Aparato Locomotor, and the Co-Director of Jornadas de Actualización en Impresión 3D Médica Hospitalaria.

JAVIER PASCAU (Member, IEEE) received the degree in telecommunication engineering from Universidad Politécnica de Madrid, in 1999, the master's degree in biomedical technology and instrumentation from Universidad Nacional de Educación a Distancia (UNED), in 2005, and the Ph.D. degree from Universidad Politécnica de Madrid, in 2006.

He is currently an Associate Professor with the Department of Bioengineering and Aerospace Engineering, Universidad Carlos III de Madrid, and a Research Fellow with the Instituto de Investigación Sanitaria Gregorio Marañón. He has authored more than 100 papers in indexed journals and conferences and one book. His research interests include multimodal image quantification and registration both in clinical and preclinical applications, surgical guidance by combining image studies and tracking systems, and machine learning methods for medical image analysis.